Efficient Biologically Inspired Photocell Enhanced by Delocalized Quantum States

C. Creatore,[1,*] M. A. Parker,[1] S. Emmott,[2] and A. W. Chin[1]

[1]*Cavendish Laboratory, University of Cambridge, Cambridge CB3 0HE, United Kingdom*

[2]*Microsoft Research, Cambridge CB1 2FB, United Kingdom*

(Received 23 July 2013; published 18 December 2013)

Artificially implementing the biological light reactions responsible for the remarkably efficient photon-to-charge conversion in photosynthetic complexes represents a new direction for the future development of photovoltaic devices. Here, we develop such a paradigm and present a model photocell based on the nanoscale architecture and molecular elements of photosynthetic reaction centers. Quantum interference of photon absorption and emission induced by the dipole-dipole interaction between molecular excited states guarantees an enhanced light-to-current conversion and power generation for a wide range of electronic, thermal, and optical parameters for optimized dipolar geometries. This result opens a promising new route for designing artificial light-harvesting devices inspired by biological photosynthesis and quantum technologies.

DOI: 10.1103/PhysRevLett.111.253601 PACS numbers: 42.50.Gy, 78.67.−n, 82.39.Jn, 84.60.Jt

Introduction.—Photosynthesis begins with an ultrafast sequence of photophysical events that convert solar photons into electrons for use in the later dark stages of the process. Remarkably, in plants, bacteria, and algae, the photon-to-charge conversion efficiency of these light reactions can approach 100% under certain conditions [1]. This suggests a careful minimization of the deleterious molecular processes, e.g., trapping, radiative, and nonradiative losses, which plague attempts to achieve similar performances in artificial solar cells [2]. Consequently, there has been long-standing and ever-increasing interest in understanding the physics of the nanoscale structures known as pigment-protein complexes (PPCs), which nature uses to drive the light reactions efficiently [3]. Recently, new insight into the energy transfer dynamics of PPCs, including the unexpected observation of coherent quantum dynamics, has been obtained from ultrafast optical experiments [4–8], creating considerable interest in the possible links between light-harvesting efficiency, the structure of quantum states supported in PPCs, and their time evolution [9–17].

Recently, Dorfman *et al.* [18] have introduced a promising approach in which the light reactions are analyzed as quantum heat engines (QHEs). Treating the light-to-charge conversion as a continuous Carnot-like cycle, Dorfman *et al.* indicate that interference effects resulting from quantum coherence could boost the photocurrent of a photocell based on photosynthetic reaction centers (RCs) by at least 27% compared to an equivalent classical photocell. In their model, the driver of this enhancement is the phenomenon of Fano interference [18–20], which enables optical systems to violate the thermodynamic detailed balance that otherwise limits the efficiency of light-harvesting devices [21].

Here, we show that much simpler dipole-dipole interactions between suitably arranged chromophores can generate quantum interference effects which can enhance photocurrents and maximum power outputs by $\gtrsim 35\%$ over a classical cell. Our device avoids using Fano interference, which is a higher-order perturbative interaction whose mathematical description in Ref. [18] appears to suffer from a number of pathologies, including the appearance of negative populations of the excited states, as documented in the Supplemental Material [22]. Our model is based on the completely positive Pauli master equation (PME), uses well understood and experimentally observed interactions, has robustness against structural variations, and could be realized and/or interfaced with other nanotechnologies inspired by biological light-harvesting structures [23].

Model.—The cyclic engine model we propose [Figs. 1(a) and 1(b)] mimics the "special pair" in photosynthetic RCs as in Ref. [18]: D_1 and D_2 represent a pair of identical and initially uncoupled donor molecules which flank an acceptor molecule A. The cycle begins with the absorption of solar photons—the whole system being initially in the ground state $|b\rangle$—leading to the population of the donor excited states $|a_1\rangle$ and $|a_2\rangle$. The excited electrons can then be transferred to the acceptor molecule (electrons being in A and holes remaining in D_1 and D_2) through electronic coupling and emission of phonons, as in Ref. [18]. Then, the charge separated state $|\alpha\rangle$ decays to a state $|\beta\rangle$ representing the now positively charged RC (the excited electron is assumed to have been used to perform work). The transfer rate Γ and steady ratio of populations between $|\alpha\rangle$ and $|\beta\rangle$ determine the current $j = e\Gamma\rho_{\alpha\alpha}$ and power output of our QHE, $\rho_{\alpha\alpha}$ being the population of $|\alpha\rangle$. We also consider the possibility of acceptor-to-donor charge recombination including the decay rate $\Gamma_{\alpha\to b} = \chi\Gamma$ [22], where χ is a dimensionless fraction. This loss channel brings the system back to the ground state but does not produce work current, and it is often a significant source of inefficiency in organic

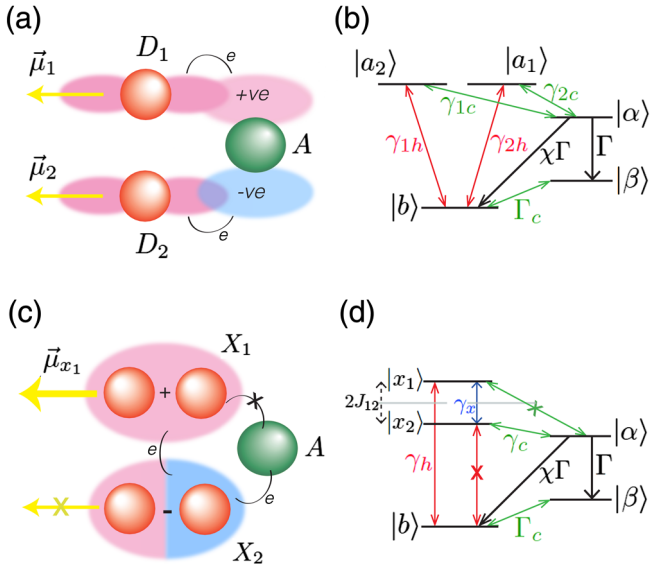

FIG. 1 (color online). Schematic of the reaction center. In (a), both donors D_1 and D_2 are optically active and contribute to transferring the excited electrons at the acceptor A. The red and blue shadowed regions surrounding the molecules denote the molecular orbitals representing the spatial distribution density of electrons. In (c), coupling between D_1 and D_2 gives rise to a coupled system (X_1, X_2) with new eigenstates: symmetric bright ($|x_1\rangle$) and antisymmetric dark ($|x_2\rangle$) superpositions of the uncoupled donor states ($|a_1\rangle$, $|a_2\rangle$). Photon emission and absorption is only possible via $|x_1\rangle$, while charge transfer to A occurs via $|x_2\rangle$ only. (b),(d) The level schemes of (a) and (c), respectively.

solar cells [24]. Finally, the cycle is closed, allowing the $|\beta\rangle$ state to decay back (via a rate Γ_c) to the neutral ground state of the system.

The new element of our scheme is the formation of new optically excitable states through strong excitonic coupling between the donors, resulting from the long-range dipole-dipole interaction [22]. Such interactions and the formation of stable delocalized exciton states are widely observed phenomena in pigment-protein complexes [3].

Within our model, we consider identical and degenerate donor excited states with parallel transition dipole moments for optical absorption and emission $|\vec{\mu}_1| = |\vec{\mu}_2| = \mu$, as shown in Figs. 1(a) and 1(b). The electron transfer matrix elements leading to charge separation have been chosen to have same magnitudes $|t_{D_1A}| = |t_{D_2A}| = t_{DA}$. Further, we exploit the possibility of using acceptor molecules hosting an electron into a lowest unoccupied molecular orbital with a spatially varying phase. For an acceptor with orbital lobes characterized by a relative phase of π [see Fig. 1(a)], placing the donor molecules close to different lobes leads to electron transfer matrix elements with the same magnitude, but opposite signs, i.e., $t_{D_2A} = -t_{D_1A}$. In the presence of dipole-dipole interactions, the eigenstates of the optically excited donor pair become coherently delocalized excitonic states. For an excitonic coupling matrix element of J_{12}, the new eigenstates are symmetric ($|x_1\rangle$) and antisymmetric ($|x_2\rangle$) combinations of the uncoupled donor states: $|x_1\rangle = 1/\sqrt{2}(|a_1\rangle + |a_2\rangle)$ and $|x_2\rangle = 1/\sqrt{2}(|a_1\rangle - |a_2\rangle)$, with corresponding eigenvalues $E_{x_1/x_2} = E_{1,2} \pm J_{12}$, $E_{1,2}$ being the energies of the uncoupled states $|a_1\rangle$ and $|a_2\rangle$, respectively, [22]. The dipole moment of $|x_1\rangle$ is therefore enhanced by constructive interference of the individual transition dipole matrix elements, $\mu_{x_1} = 1/\sqrt{2}(\mu_1 + \mu_2) = \sqrt{2}\mu$, whereas the dipole moment of $|x_2\rangle$ cancels due to destructive interference. Hence, the symmetric combination describes an optically active bright state with a photon absorption and emission rate $\gamma_h \propto |\mu_{x_1}|^2 = 2|\mu|^2$, which is twice that of the uncoupled donor states ($\gamma_{1h} = \gamma_{2h} \propto |\mu|^2$), while the antisymmetric combination describes an optically forbidden dark state. Crucially for our scheme, the bright state lies $2J_{12}$ higher in energy compared to the dark state. Similarly, the bright state has a resultant charge transfer matrix element equal to zero and the dark state has a matrix element $t_{x_2A} = \sqrt{2}t_{DA}$, giving an enhanced electron transfer rate $\gamma_c \propto |t_{x_2A}|^2 = 2|t_{DA}|^2$, i.e., twice the rate of the uncoupled donors $\gamma_{1c} = \gamma_{2c} \propto |t_{DA}|^2$. These excitonic modifications of the matrix elements (and consequently the transfer rates) are, ultimately, the key to producing higher photocurrent power in our cell compared to uncoupled chromophores.

With this scheme, the photon absorption and electron transfer parts of the cycle are disconnected unless there is population transfer between the bright and dark states. This is provided by the phonon-mediated energy relaxation, which can be very effective between excitonic systems with strong pigment overlap [3]. This is included in our kinetic model via the relaxation rate γ_x [Fig. 1(d)]. Following the standard interpretation of most experimental studies of PPCs and molecular chromophores, we assume that the new donor states induced by the excitonic coupling are directly populated by the absorption of weak incoherent solar photons. Therefore, treating the donor-light, electron transfer, and bright-dark relaxation couplings in second-order perturbation theory, the kinetics of the optically excited states obeys the following PME, which is guaranteed to give completely positive populations:

$$\begin{aligned}
\dot{\rho}_{a_1a_1} &= -\gamma_{1h}[(1+n_{1h})\rho_{a_1a_1} - n_{1h}\rho_{bb}] \\
&\quad - \gamma_{1c}[(1+n_{1c})\rho_{a_1a_1} - n_{1c}\rho_{\alpha\alpha}], \\
\dot{\rho}_{a_2a_2} &= -\gamma_{2h}[(1+n_{2h})\rho_{a_2a_2} - n_{2h}\rho_{bb}] \\
&\quad - \gamma_{2c}[(1+n_{2c})\rho_{a_2a_2} - n_{2c}\rho_{\alpha\alpha}],
\end{aligned} \tag{1}$$

$$\begin{aligned}
\dot{\rho}_{x_1x_1} &= -\gamma_x[(1+n_x)\rho_{x_1x_1} - n_x\rho_{x_2x_2}] \\
&\quad - \gamma_h[(1+n_h)\rho_{x_1x_1} - n_h\rho_{bb}], \\
\dot{\rho}_{x_2x_2} &= \gamma_x[(1+n_x)\rho_{x_1x_1} - n_x\rho_{x_2x_2}] \\
&\quad - \gamma_c[(1+n_{2c})\rho_{x_2x_2} - n_{2c}\rho_{\alpha\alpha}].
\end{aligned} \tag{2}$$

In Eqs. (1) and (2), n_{1h} (n_{2h}) and n_h are the average numbers of photons with frequencies matching the transition energies from the ground state to $|a_1\rangle$ ($|a_2\rangle$) and $|x_1\rangle$, respectively; n_{1c} (n_{2c}) are the thermal occupation numbers of ambient phonons at temperature T_a with energies $E_1 - E_\alpha$ ($E_2 - E_\alpha$) for $J_{12} = 0$ [Eq. (1)] and $E_{x_1} - E_\alpha$ ($E_{x_2} - E_\alpha$) for $J_{12} \neq 0$ [Eq. (2)]; and n_x is the corresponding thermal occupation at T_a with energy $E_{x_1} - E_{x_2}$. The rates in Eqs. (1) and (2) obey local detailed balance and correctly lead to a Boltzmann distribution for the level populations if the thermal averages for the photon and phonon reservoirs are set to a common temperature. We consider the fully populated ground state, i.e., $\rho_{bb}(t = 0) = 1$, as the initial condition. The full PME and further details of the excitonic Hamiltonian and the effective matrix elements of the delocalized states are given in the Supplemental Material [22]. Finally, before presenting our results, we point out that natural RCs and Photosystem II do not have their special-pair dipole moments in the parallel arrangement we shall explore. However, our goal is to explore how the same molecular resources could be more profitably arranged to extract power in a model or nanofabricated cell, and in the Supplemental Material, we show that the geometry here considered is optimal for photoconversion [22]. Therefore, we focus on this case in the rest of this Letter. We also do not consider the role of dynamical intereigenstate coherences, first because populations and coherences are uncoupled in secular Redfield theory and second because recent findings [25,26] suggest that under the operational conditions of our proposed photocell, i.e., weak incoherent illumination by sunlight, these coherences are unlikely to even be generated at all.

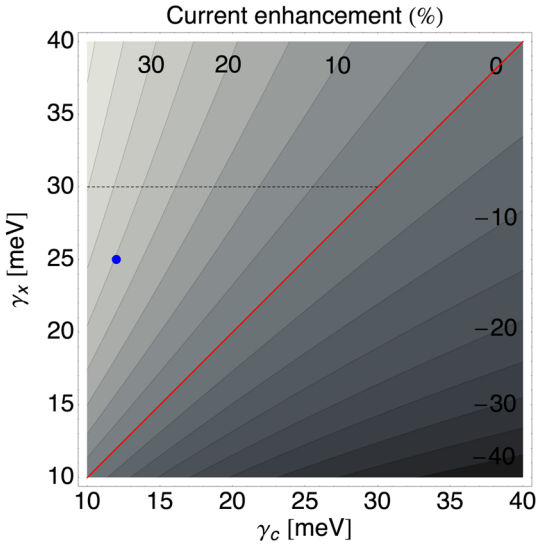

FIG. 2 (color online). Contour plot of the percentage current enhancement $(j - \tilde{j})/\tilde{j}$ calculated as a function of the phonon rates γ_x and γ_c at $T_a = 300$ K. The thick red line $\gamma_x = \gamma_c$ denotes the zero-enhancement region. The dashed black line $\gamma_x = 2J_{12} = 30$ meV marks the upper limit for γ_x. The blue dot shows the enhancement ($\sim 25\%$) when $\gamma_x = 25$ meV and $\gamma_c = 12$ meV.

Results.—Figure 2 shows the relative enhancement $(j - \tilde{j})/\tilde{j}$, j and $\tilde{j}$ being the electric current in the excitonically coupled ($J_{12} \neq 0$) and uncoupled ($J_{12} = 0$) cases, respectively, when the system reaches steady-state operation—see the Supplemental Material [22]. The current enhancement has been evaluated at room temperature as a function of the transition rates γ_x and γ_c ($= \gamma_{1c} + \gamma_{2c}$ with $\gamma_{1c} = \gamma_{2c}$) using realistic photon decay rates and average numbers of solar concentrated photons and ambient phonons as listed in Table I and reported in Ref. [18]. We have here considered a modest recombination rate $\Gamma_{\alpha\to b} = \chi\Gamma$ with $\chi = 20\%$, while results for a wider range of χ values can be found in Ref. [22]. Interestingly, it is shown that the relative enhancement of photocurrent is actually slightly larger for strong recombination, although the overall current is lower for faster recombination. When $\gamma_x = \gamma_c$ (see the thick continuous red line in Fig. 2), there is no enhancement as $j = \tilde{j}$: charge transfer via the channel $x_1 \to x_2 \to \alpha$ is as fast as the combined transfer through the independent channels $a_1 \to \alpha$ and $a_2 \to \alpha$. However, when $\gamma_x > \gamma_c = \gamma_{1c} + \gamma_{2c}$, coherent coupling leads to substantial current enhancements as compared to the configuration without coupling (see the region $\gamma_x > \gamma_c$ in Fig. 2). These positive enhancements increase monotonically with increasing γ_x. This results from the new delocalized level structure, which introduces an effective shelving state—the dark state—into the cycle. This allows the deleterious photonic emission from the bright state to be outcompeted by the fast bright-to-dark relaxation. Then, as emission losses are absent in the dark state, all its population must pass through the work (extracting) stage. Further, when $\gamma_x > \gamma_c$, the absorbed solar energy can be removed faster than the absorbers in the incoherent case can move it to the acceptor $|\alpha\rangle$ state. Hence, the enhancements result from the creation of an irreversible valve through which solar energy is quickly extracted and stably stored to build up higher voltages or driving forces to extract power in the latter part of the cycle [27].

We have assumed that the delocalized states formed through the dipolar coupling are stable under the

TABLE I. Parameters used in the numerical simulations.

	Energies and decay rates (eV)	Occupation numbers
$E_1 - E_b = E_2 - E_b$	1.8	
$E_1 - E_\alpha = E_2 - E_\alpha = E_\beta - E_b$	0.2	
J_{12}	0.015	
$\gamma_h = 2\gamma_{1h} = 2\gamma_{2h}$	1.24×10^{-6}	
Γ	0.124	
Γ_c	0.0248	
n_x		0.46
$n_h = n_{1h} = n_{2h}$		60 000

steady-state operation, whereas the dephasing of these states, due to energy relaxation, may suppress their phase coherence. Employing the standard condition, that the superposition states will be stable provided that $2J_{12} > \gamma_x$ [28], the achievable enhancement in conditions related to the parameters of Table I is restricted to 35% (see the dashed black line $\gamma_x = 2J_{12} = 30$ meV in Fig. 2). Larger enhancements can be achieved by either decreasing γ_c or increasing γ_x. However, smaller γ_c monotonically reduces the generation of current at the acceptor, whereas, as $2J_{12} > \gamma_x$, larger couplings allow larger γ_x and greater currents.

The excitonic coupling in Table I, corresponding to a splitting of $\approx 240\ \mathrm{cm}^{-1}$, is actually towards the lower end of the typical excitonic splittings in natural RCs (200–$800\ \mathrm{cm}^{-1}$) [18], suggesting that even larger enhancements could be possible. Moreover, splittings much larger than thermal energy at room temperature ($k_b T_a \approx 210\ \mathrm{cm}^{-1}$) cause the bright to the dark state transitions to become essentially unidirectional. This minimizes the thermal repopulation of the bright state and thus the emissive losses to the ground state, an effect which can also be obtained by the decreasing the cell's ambient temperature [22].

Within this scheme, the current generated can be thought to flow across a load connecting the acceptor levels α and β. The voltage V across this load can be expressed as $eV = E_\alpha - E_\beta + k_b T_a \ln(\rho_{\alpha\alpha}/\rho_{\beta\beta})$, e being the electric charge [2,18,27]. The performance of our RC-inspired QHE can be thus assessed in terms of its photovoltaic properties, calculating the steady-state current-voltage ($j - V$) characteristic and power generated. The $j - V$ characteristic and power $P = j \cdot V$ are evaluated using the steady-state solutions of the PME, calculated at increasing rate Γ at fixed other parameters: from $\Gamma \to 0$ ($j \to 0$), corresponding to the open circuit regime where $eV = eV_{\mathrm{oc}} = (E_{a_1/x_1} - E_b)(1 - T_a/T_S) \approx E_{a_1/x_1} - E_b$, to the short circuit regime where $V \to 0$. The $j - V$ and the $P - V$ behaviors are shown in Fig. 3 for both cases of coupled ($J_{12} \neq 0$) and uncoupled ($J_{12} = 0$) donors. Using the parameters listed in Table I with $\gamma_c = 12$ meV and $\gamma_x = 25$ meV (see Fig. 2), we get a peak current enhancement $\approx 25\%$. The enhancement of the delivered peak power in the presence of coherent coupling is quantified by defining the relative efficiency $\eta_R = (P_{\mathrm{out}}^{\mathrm{max}} - \tilde{P}_{\mathrm{out}}^{\mathrm{max}})/\tilde{P}_{\mathrm{out}}^{\mathrm{max}}$, $P_{\mathrm{out}}^{\mathrm{max}}$ and $\tilde{P}_{\mathrm{out}}^{\mathrm{max}}$ being the output peak powers with ($J_{12} \neq 0$) and without ($J_{12} = 0$) coupling, respectively. For the parameters used in the simulation shown in Fig. 3, $\eta_R \approx 25\%$. The coherent RC-based photocell thus generates higher peak powers by drawing a larger current and energy flux from the same available solar radiation source while maintaining the same voltage. Furthermore, for decreasing temperatures, the efficiency of charge transfer increases and improved photocell performances with η_R up to 40% can be achieved [22].

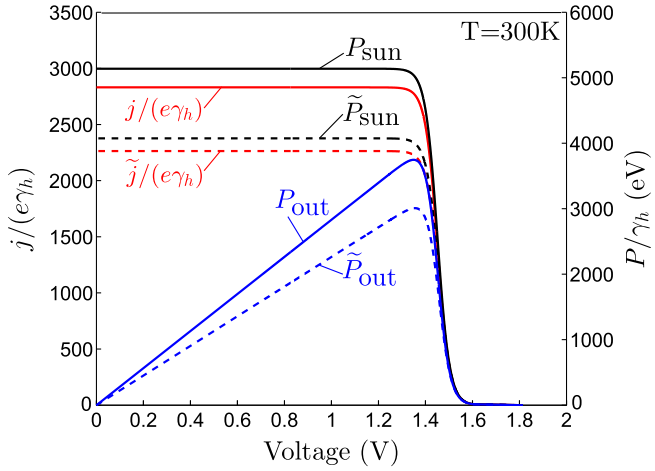

FIG. 3 (color online). Current and power generated as a function of the induced cell voltage V at room temperature. The thin continuous red (j/e, $J_{12} \neq 0$) and dashed ($\tilde{j}/e$, $J_{12} = 0$) lines represent the dimensionless current. The power generated as a function of the cell voltage is indicated by thin continuous blue (P_{out}, $J_{12} \neq 0$) and dashed ($\tilde{P}_{\mathrm{out}}$, $J_{12} = 0$) lines; the power acquired from the Sun is indicated by the thick continuous black [$P_{\mathrm{Sun}} = j(E_{x_1} - E_b)/e$, $J_{12} \neq 0$] and dashed [$\tilde{P}_{\mathrm{Sun}} = \tilde{j}(E_{a_1} - E_b)/e$, $J_{12} = 0$] lines.

Conclusions.—The possibility for harnessing quantum effects such as the formation of coherent superpositions has been previously highlighted in the context of energy transfer in PPCs [9–17], and this fascinating potential may soon be realized in artificial molecular light-harvesting systems, such as those recently synthesised by Hayes *et al.* [29]. For these applications, advanced simulation techniques [16,30–36] will be required to assess the optimal design and stability of the engineered quantum states, including details of additional states, e.g., charge transfer states [30,36], in PPC-like or organic materials. Another potential direction, requiring different theoretical tools, involves the use of solid-state chromophores: quantum dots, superconducting qubits, plasmonic nanostructures, and possibly hybrid combinations of the above [23,37].

A. W. C. acknowledges support from the Winton Programme for the Physics of Sustainability; C. C. acknowledges support from the EPSRC. We would like to thank Nick Hine and Akshay Rao for useful discussions.

*cc619@cam.ac.uk

[1] R. E. Blankenship, *Molecular Mechanisms of Photosynthesis* (Blackwell Science Ltd, Oxford, UK, 2002).
[2] P. Wurfel, *Physics of Solar Cells* (Wiley-VCH, Berlin, 2009).
[3] H. van Amerongen, L. Valkunas, and R. van Grondelle, *Photosynthetic Excitons* (World Scientific, Singapore, 2000).
[4] G. S. Engel, T. R. Calhoun, E. L. Read, T.-K. Ahn, T. Mančal, Y.-C. Cheng, R. E. Blankenship, and G. R. Fleming, Nature (London) **446**, 782 (2007).

[5] T. R. Calhoun, N. S. Ginsberg, G. S. Schlau-Cohen, Y.-C. Cheng, M. Ballottari, R. Bassi, and G. R. Fleming, J. Phys. Chem. B **113**, 16 291 (2009).
[6] G. Panitchayangkoon, D. Hayes, K. A. Fransted, J. R. Caram, E. Harel, J. Wen, R. E. Blankenship, and G. S. Engel, Proc. Natl. Acad. Sci. U.S.A. **107**, 12 766 (2010).
[7] D. Hayes, G. Panitchayangkoon, K. A. Fransted, J. R. Caram, J. Wen, K. F. Freed, and G. S. Engel, New J. Phys. **12**, 065042 (2010).
[8] E. Collini, C. Y. Wong, K. E. Wilk, P. M. G. Curmi, P. Brumer, and G. D. Scholes, Nature (London) **463**, 644 (2010).
[9] M. B. Plenio and S. F. Huelga, New J. Phys. **10**, 113019 (2008).
[10] M. Mohseni, P. Rebentrost, S. Lloyd, and A. Aspuru-Guzik, J. Chem. Phys. **129**, 174106 (2008).
[11] A. Olaya-Castro, C. F. Lee, F. F. Olsen, and N. F. Johnson, Phys. Rev. B **78**, 085115 (2008).
[12] F. Caruso, A. W. Chin, A. Datta, S. F. Huelga, and M. B. Plenio, J. Chem. Phys. **131**, 105106 (2009).
[13] P. Rebentrost, M. Mohseni, I. Kassal, S. Lloyd, and A. Aspuru-Guzik, New J. Phys. **11**, 033003 (2009).
[14] A. W. Chin, A. Datta, F. Caruso, S. F. Huelga, and M. B. Plenio, New J. Phys. **12**, 065002 (2010).
[15] H. Dong, D.-Z. Xu, J.-F. Huang, and C.-P. Sun, Light: Sci. Appl. **1**, e2 (2012).
[16] A. W. Chin, J. Prior, R. Rosenbach, F. Caycedo-Soler, S. F. Huelga, and M. B. Plenio, Nat. Phys. **9**, 113 (2013).
[17] M. d. Rey, A. W. Chin, S. F. Huelga, and M. B. Plenio, J. Phys. Chem. Lett. **4**, 903 (2013).
[18] K. E. Dorfman, D. V. Voronine, S. Mukamel, and M. O. Scully, Proc. Natl. Acad. Sci. U.S.A. **110**, 2746 (2013).
[19] M. O. Scully, K. R. Chapin, K. E. Dorfman, M. B. Kim, and A. Svidzinsky, Proc. Natl. Acad. Sci. U.S.A. **108**, 15 097 (2011).
[20] A. A. Svidzinsky, K. E. Dorfman, and M. O. Scully, Phys. Rev. A **84**, 053818 (2011).
[21] W. Shockley and H. J. Queisser, J. Appl. Phys. **32**, 510 (1961).
[22] See Supplemental Material at http://link.aps.org/supplemental/10.1103/PhysRevLett.111.253601 for details about the model we developed and comparison with previous related work.
[23] K. D. B. Higgins, S. C. Benjamin, T. M. Stace, G. J. Milburn, B. W. Lovett, and E. M. Gauger, arXiv:1306.1483.
[24] J.-L. Bredas, J. E. Norton, J. Cornil, and V. Coropceanu, Acc. Chem. Res. **42**, 1691 (2009).
[25] P. Brumer and M. Shapiro, Proc. Natl. Acad. Sci. U.S.A. **109**, 19 575 (2012).
[26] I. Kassal, J. Yuen-Zhou, and S. Rahimi-Keshari, J. Phys. Chem. Lett. **4**, 362 (2013).
[27] O. D. Miller, E. Yablonovitch, and S. R. Kurtz, IEEE J. Photovoltaics **2**, 303 (2012).
[28] A. Shnirman, Y. Makhlin, and G. Schön, Phys. Scr. **T102**, 147 (2002).
[29] D. Hayes, G. B. Griffin, and G. S. Engel, Science **340**, 1431 (2013).
[30] V. I. Novoderezhkin, A. G. Yakovlev, R. van Grondelle, and V. A. Shuvalov, J. Phys. Chem. B **108**, 7445 (2004).
[31] J. Prior, A. W. Chin, S. F. Huelga, and M. B. Plenio, Phys. Rev. Lett. **105**, 050404 (2010).
[32] A. W. Chin, A. Rivas, S. F. Huelga, and M. B. Plenio, J. Math. Phys. (N.Y.) **51**, 092109 (2010).
[33] V. Balevičius, Jr., A. Gelzinis, D. Abramavicius, T. Mančal, and L. Valkunas, Chem. Phys. **404**, 94 (2012).
[34] A. Ishizaki and G. R. Fleming, J. Chem. Phys. **130**, 234111 (2009).
[35] P. Nalbach, D. Braun, and M. Thorwart, Phys. Rev. E **84**, 041926 (2011).
[36] A. Gelzinis, L. Valkunas, F. D. Fuller, J. P. Ogilvie, S. Mukamel, and D. Abramavicius, New J. Phys. **15**, 075013 (2013).
[37] R. A. Shah, N. F. Scherer, M. Pelton, and S. K. Gray, Phys. Rev. B **88**, 075411 (2013).